

We are IntechOpen, the world's leading publisher of Open Access books Built by scientists, for scientists

6,900

Open access books available

186,000

International authors and editors

200M

Downloads

Our authors are among the

154

Countries delivered to

TOP 1%

most cited scientists

12.2%

Contributors from top 500 universities



WEB OF SCIENCE™

Selection of our books indexed in the Book Citation Index
in Web of Science™ Core Collection (BKCI)

Interested in publishing with us?
Contact book.department@intechopen.com

Numbers displayed above are based on latest data collected.
For more information visit www.intechopen.com



SCIROCCO Plasma Wind Tunnel: Synergy between Numerical and Experimental Activities for Tests on Aerospace Structures

Rosario Borrelli and Adolfo Martucci
*Italian Aerospace Research Center – CIRA
Italy*

1. Introduction

Spacecraft structures are subjected to aerodynamic heating during launch and re-entry phases of their operations. The design of these structures poses several challenges to structural designer since the aerodynamic heating, which is the predominant load (Kelly et al., 1983; Shih et al., 1988), induces elevated temperatures that can affect the structural behaviour in several harmful ways: degradation of the elastic material properties, reduction of allowable stresses and generation of high thermal stress due to restrained local thermal expansion/contractions.

The success of a re-entry spatial mission in the Earth atmosphere, as well known, is strongly related to the performances of the Thermal Protection Systems (TPSs), which play the most important role (Thornton, 1996). The TPS is the most critical component of a spacecraft since if they are somehow damaged during the mission, a chain reaction can be triggered, leading to a quick propagation of the damage on the whole structure, inestimable economic losses and, above all, losses of human lives. The task of a TPS is to protect the substructure of the vehicle against local and global overheating. In order to ensure the feasibility of interplanetary missions, and in general for the qualification of the critical parts of reentry vehicles, TPS concepts have to be first qualified on-ground and then tested and validated in flight conditions. Thus, Plasma Wind Tunnel facilities have a key role during this qualification process. They should be able to simulate hypersonic air flows encountered during re-entry into Earth atmosphere and to test TPS concepts on full scale demonstrator.

Nevertheless, reproducing hypersonic conditions in the wind tunnels is harder, if not impossible, with respect to other motion conditions. As matter of fact, it is very complicated to reproduce simultaneously the enthalpy, the hypersonic speed, the chemical composition of gases and the dimensions of the model, which are the main factors which characterize the motion.

As a consequence, a choice is needed between wind tunnels designed for the aerodynamic simulation and those ones designed for the thermal simulation.

2. Plasma wind tunnels in the world

Thus, wind tunnels can be classified in two categories:

- Aerodynamic, for the simulation of the Mach number;

- Aero-thermodynamic, for the simulation of heat fluxes.

The main feature of the “blow down” aerodynamic wind tunnels is that to reach high Mach numbers it is needed to pre-heat the air before the expansion through a nozzle. In this kind of wind tunnels, the flux is characterized by a very high stagnation pressure which is indispensable to obtain elevated Mach numbers. The duration of the tests is rather limited because it is related to the emptying time of the tank. Typically, they last some dozens of seconds. The aerodynamic wind tunnels work in an intermitting fashion since it is needed to wait for a certain time to recompress the fluid, in such a time the wind tunnel is inactive.

On the other hands, the aerothermo-dynamic wind tunnels are mainly fed by an electric arc and they work in a continuous fashion. The gas heated by the arc reaches very high temperature. Such kind of wind tunnels are mainly used to reproduce heat fluxes in order to test the performances of ablative materials or TPSs, as well as to investigate aerothermo-chemical problems. In the aero-thermodynamic wind tunnels, it is very complicated to determine the thermo-fluid dynamic parameters such as Mach, Reynolds, Knudsen numbers and so on.

One of the most crucial difficulty is that after the gas has been heated by the arc-heater and has passed through the nozzle, its composition is unknown and sophisticated diagnostics techniques are needed to evaluate it. Numerical models are also conveniently used to predict the gas thermo-chemical evolution and to characterize the fluid in the test chamber.

2.1 SCIROCCO plasma wind tunnel

In the mid eighties the European Space Agency (ESA) feels the need of an appropriate facility to carry out experimental ground tests. The intention was to realize a wind tunnel with high enthalpy and very large dimensions so that full scale component of spacecrafts could be tested. Indeed, in hypersonic conditions, the heat fluxes distribution is affected by the sizes of the model.

Since Italy was very interested to the project, the conceptual design, the feasibility study and the preliminary design activities were assigned to the Italian Aerospace Research Centre (CIRA) and were performed between the 1988 and 1989.

In that period was noticed the need to have stagnation temperatures close to 10000 K. Hence, such a value was used to define the technical specifications of the arc-heater.

The air flux in the wind tunnel should be characterized by very high temperature and for this reason, the name “Scirocco”, which is the warm wind coming from the Sahara Desert and acting on the Mediterranean coasts, was given to the facility.

The final design started in observance to a grant agreement between ESA and the Italian Ministry of University and Scientific and Technologic Research (MURST).

The facility started to be built in December 1994 and the work finished in 2001.

As shown in Figure 1, Scirocco is the largest arc jet test facility in the world in terms of arc heater power (about 70 MW).

Moreover, a nozzle with a 2 metre diameter exit allows full-scale models of space-vehicle thermal protection systems to be tested for up to 30 minutes, a period which corresponds to the duration of re-entry. The facility, providing thermal energy to the gas, is able to generate an elevated massive flow and very high temperature, allowing hypersonic conditions to be easily reproduced. The peculiar characteristics of the hypersonic regime, extensively described above, make the requirements of the test to be very constrained.

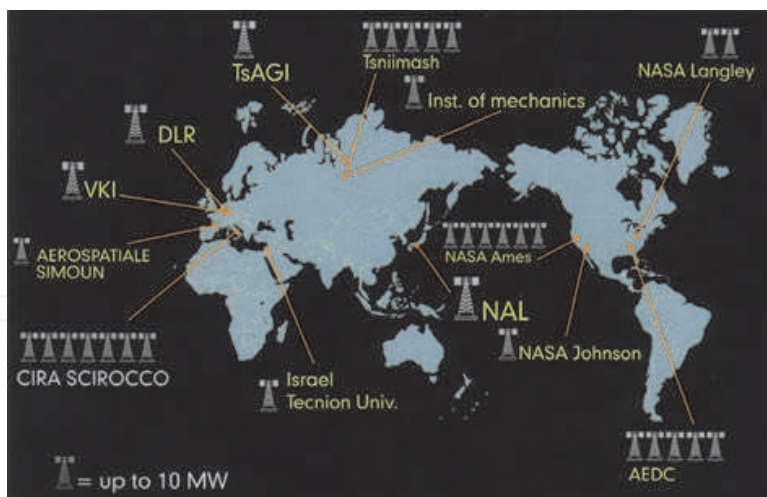


Fig. 1. Plasma wind tunnels in the world

The Scirocco PWT is used in the field of aerospace technology development and its main applications can be summarized as follows:

- Investigate aerothermodynamic phenomena related to the re-entry of both space vehicles and capsules: this is the primary use, indeed Scirocco is able to simulate the re-entry trajectory of several space vehicles, e.g. the Space Shuttle.
- Investigate the aerothermodynamic of launch vehicles during the ascending phase: problems related to the aerodynamic heating raise also in the launch phase and they are caused by the high acceleration values; such problems are similar to those ones induced by the re-entry with the difference that in this case the heating occurs in a lower atmosphere characterized by a higher value of the air density.
- Investigation on exhaust nozzles for launch vehicles and missiles.
- Investigation on the aerothermochemical of internal fluxes: such an analysis is aimed at developing of aerospace propulsion systems (ramjet, scramjet)
- Study on the interaction between the plasma and the electromagnetic fields: in particular, the communications black-out between the ground and the vehicles occurring during the re-entry phase is investigated.
- Study on industrial processes which induce a variation of the chemical composition of the used gas.

A typical test performed in the SCIROCCO wind tunnel can be sketched as shown in Figure 2 where the different phases are outlined.

An air mass flow rate varying between 0.1 and 3.5 Kg/s and with a pressure of 87 bar is supplied by a compression system and then is introduced in the arc heater together with a little argon mass flow rate which is used to help the arc heater ignition and to reduce the oxidation of the electrodes.

Once the arc heater reaches the steady state conditions, it converts the electric energy in the thermal one, thus increasing the air temperature.

The electrodes receive the electric energy which is provided by a Power Supply System. Such system converts the alternate current, coming from the external power supply, in direct current. Inside the arc heater, the air reaches pressures varying between 1 and 17 bar and temperatures varying between 2000 and 10000K. Successively, the air is expanded through a conical nozzle and crosses the test chamber at the thermodynamic conditions required by the test.

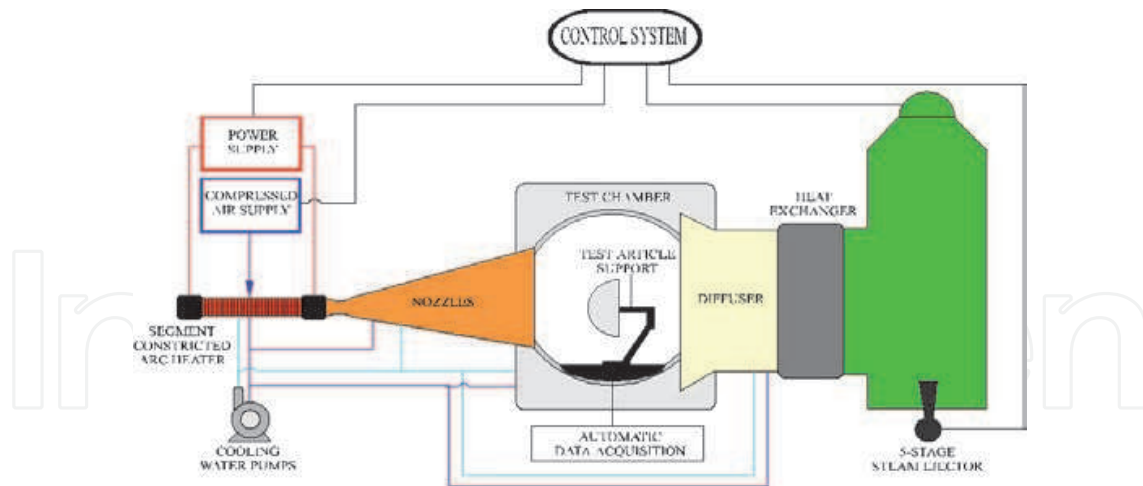


Fig. 2. Sketch of a typical test performed at the SCIROCCO Plasma wind tunnel

After that, the test article is inserted in the plasma flow by means of an automatic robot which is named Model Support System (MSS) fixed to the base of the test chamber. The main physical parameters are monitored by means of a Data Acquisition System (DAS). Advanced instrumentations are installed both inside and outside the test chamber.

The plasma flow is then collected in the diffuser whose main task is to reduce the plasma speed from supersonic values to subsonic ones. The diffuser is made by a convergent-divergent horizontal nozzle with a long central part at uniform section and it is cooled by an external cooling system.

At the end of diffuser, the air flow encounters the heat exchanger which reduces the temperature of the air consistently with the thermal strength of the materials used for the vacuum system which is located afterwards. The vacuum system generates and keeps the vacuum conditions required by the test. All the components located between the arc heater and the heat exchanger identify the SCIROCCO Test Leg.

A system, named "DeNOx" system, follows the vacuum system and its aim is to reduce the amount of nitrogen oxide produced in the Test Leg during the test.

In order to reduce the thermal energy produced in the various components of the Test Leg a water cooling system is used. Two water cooling circuits are used with two different values of the water pressure. In both the water is demineralised for two reasons, first, to avoid the salt deposition along the exchange surfaces which may reduce the heat exchange coefficients, and second, to avoid problems related to the electric conductivity of non demineralised water. The high pressure circuit is used to cool critical component of the Test Leg where very high heat exchange coefficients are needed, the other components are cooled by the low pressure circuit. Moreover, cooling water is used both to cool some components of the facilities and to decrease the temperature of the demineralised water.

The SCIROCCO PWT has an advanced control and automation system, able to reproduce with a good accuracy the re-entry trajectory of space vehicles. Every subcomponent has a dedicated Local Central Unit (LCU) which monitors the process from an operative and safety point of view. The LCUs are connected each other and are also connected to a Central Computer System (CCS) which acts as supervisor of the whole facility. The connection between all the components is made through an high velocity transmission system.

The operating envelope of the SCIROCCO PWT, in terms of plasma total pressure and enthalpy which can be obtained in the test chamber, is shown in Figure 3.

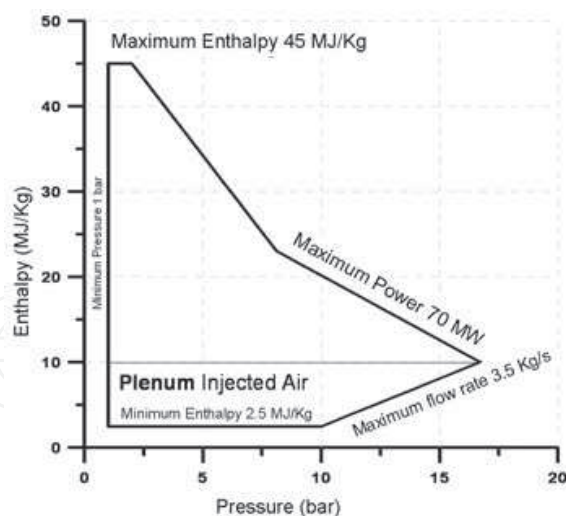


Fig. 3. Operating envelope of the SCIROCCO PWT

It was obtained by taking into account the operating and technological limits of the facilities which can be summarized as follows:

- Minimum allowable power provided by the Power Supply System equal to 1 MW;
- Minimum air pressure able to make steady the arc heater equal to 1 bar;
- Maximum allowable total enthalpy of the gas equal to 45 MJ/Kg
- Maximum direct current value equal to 9000 A;
- Maximum allowable heat flux at the nozzle groove equal to 5 KW/cm²;
- Maximum allowable power provided by the Power Supply System equal to 70 MW;
- Maximum air massive flow equal to 3.5 kg/s;
- Minimum allowable total enthalpy of the gas equal to 2.5 MJ/Kg

In the next paragraph, the main components of the whole facility is described in detail.

2.1.1 The arc heater

The arc heater installed at the SCIROCCO PWT is the largest of its kind in the world. It is located between the air compressor system and the nozzle and its main task is to heat the air by converting electric energy in thermal one. Such conversion is activated by a spark which is generated between an anode and a cathode having different electric potentials.

The arc heater shown in Figure 4, is made of a column 5500mm long, with an internal diameter of 110 mm. The anode and the cathode, each one made of 9 electrodes, are located at the two ends of the columns. The electric current is provided by a power cabin and the ballast resistors, which uniformly canalize the current, are installed before the electrodes.

In Table 1, the arc heater design technical specifications are reported.

The arc heater structure is divided into several blocks (in order to optimize the phase of maintenance and the cooling) and each single block consists of several discs inside which there is the passage of demineralised water at high pressure for the cooling (used because, as said, the absence of minerals makes it not electrically conductive), and compressed air coming from the external line. The air and water ducts that enter the individual blocks have different colours, and both the inlet pressure demineralised water, and the compressed air pressure vary along the length of the arc depending on the areas that need more cooling.

The anode is made of a copper alloy that resists to high thermo-mechanical stresses and it is connected with the power lines coming from the power unit.

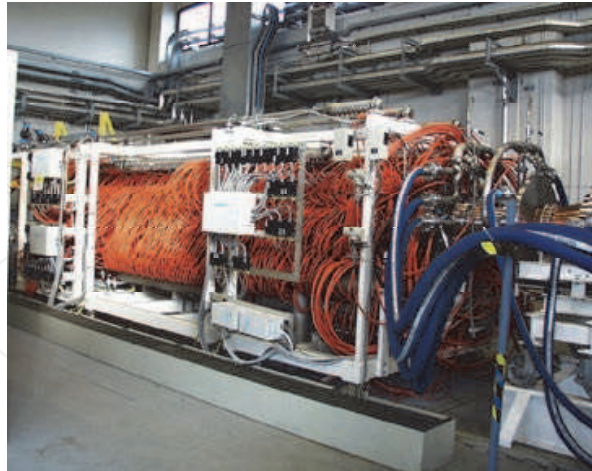


Fig. 4. Arc heater

	Min	Max
Air pressure (bar)	1	16.7
Air mass flow rate (kg/s)	0.1	3.5
Enthalpy (MJ/kg)	2.5	45
Electrical power (MW)	1	70
Electrical current (A)	1000	9000
Voltage (V)	1000	30000

Table 1. Arc heater design technical specifications

In the anode high pressure argon is introduced whose primary purpose is to avoid a direct contact between the electrodes and the flow of electrons, thereby avoiding a localized corrosion of the inside of the electrodes which obviously would cause serious problems. The second purpose related to the use of argon is to help the ignition of the arc, since it increases the conductivity of the air flow. The cathode has a configuration similar to the anode and it is at the other end of the arc.

The column is inserted between the anode and the cathode. As mentioned, it has a maximum length of 5500 mm and a variable configuration (it consists of 28 members each in turn composed of 20 rings) depends on the enthalpy level required.

The column is designed to confine the plasma as possible along the axial direction and to avoid problems of corrosion and melting of materials. Between the rings there is a layer of insulator (spacer) and both demineralised water and air, which is fed into the column with a velocity component tangential to the duct, enter. Following this tangential velocity is going to settle with the axial velocity component coming from the vacuum created by the vacuum system, generating a spiral motion.

It should be noted that a part of the flow remains attached to the inner walls of the column, creating a sort of gap that prevents the fusion of this.

Inside the column there is the motion of electrons from anode (high potential) to cathode (low potential) submitted to the Lorentz force. In this phase the conversion of electrical energy into heat energy takes place, because the electrons collide with the moving particles of air and argon, heating for viscous friction and energizing the flow.

As the temperature increases to levels high enough to trigger such vibration and dissociation of molecules and ionization of atoms the gas becomes "plasma".

Immediately downstream of the cathode there is the plenum, which has a constant cross section of 172 mm and is essentially intended to lower the total enthalpy of the air below the limit imposed by the minimum value of electric current. This is done by injecting air into this section at room temperature, which generates a resulting reduction in temperature of the plasma which, of course, will change its chemical composition.

2.1.2 Conical nozzle

The nozzle is composed of a convergent-divergent duct that has the function to expand the flow by increasing the speed and reducing the static pressure, in order to obtain the required thermo-fluid dynamic test conditions. Table 2 shows the nozzle design specifications:

	Min	Max
Inlet pressure (bar)	1	16.7
Outlet pressure (mbar)	0.01	2.9
Inlet velocity (m/s)	120	350
Outlet velocity (m/s)	2000	7000

Table 2. Design requirements for the nozzle

The first part of this component is a convergent trait in which the motion is subsonic. In the throat (i.e., the minimum diameter section, which in this case is 75 mm), the Mach reaches the unit value, and in the divergent part a further expansion occurs up to supersonic Mach numbers in the output section. The mach depends on the configuration of the nozzle used.

In fact it is divided into seven parts with different diameters of the output section, which allow to configure the nozzle so as to achieve different test conditions. As noted in Table 3, the maximum diameter of the outlet section is equal to 1950 mm, which corresponds to a ratio of the areas (outlet area divided by the area of the throat) equal to 676.

	Length (mm)	Inlet diameter (mm)	Outlet diameter (mm)
Throat section	560	170	188
Expansion section A	692	188	432
Expansion section B	692	433	677
Expansion section C	638	678	900
Expansion section D	1347	678	1150
Expansion section E	1914	678	1350
Expansion section F	1701	1350	1950

Table 3. Nozzle configurations

The critical part in terms of thermo-mechanical stress is the throat where very high temperature can be reached. In fact, while the entire nozzle is cooled with demineralised water at low pressure (which runs in conduits placed lengthwise along the outer surface),

the throat is cooled by demineralised water pipes dedicated at high pressure through a mechanism that guarantees a higher forced convection heat transfer coefficient.

At the nozzle exit, then, there are four sensors that follow the evolution of static pressure.

2.1.3 Test chamber

The Test Chamber (TC) has a cylindrical shape (Figure 5) and it is the place where the flow field to be simulated is realized (Figure 6). In fact, inside it the plasma coming from the nozzle impacts the model and the experimental measurements of pressure and temperature are carried out. Such measurements, properly treated, represent the ultimate goal of the entire system.



Fig. 5. Test chamber

The test chamber is 9217 mm high and has an inner diameter of 5170 mm, it has three openings necessary to allow the entrance to the maintenance staff and to allow to do the assembly on the support of the model, it also has a number of side windows to allow monitoring and diagnostics of the plasma flow. This component has a sliding floor to the entrance of the model and is not cooled.

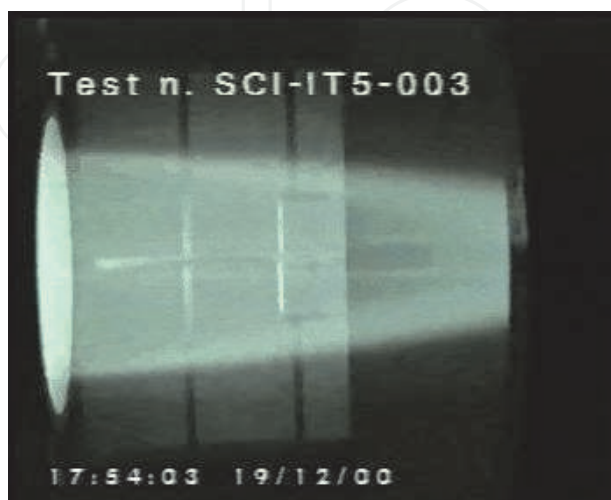


Fig. 6. Plasma flow inside the Test Chamber.

During a test performed under special conditions, such as a low flow, it is possible to inject inside the test chamber a small amount of air called "bleed air" in order to increase the value of chamber pressure and limiting the recirculation of plasma.

In the test chamber, static pressure meters and temperature meters are located at various points, moreover, two tools called "probes" are introduced within the plasma flow before the entry of the support model.

The purpose of this process is monitoring the status of thermo-fluid dynamic conditions of plasma in terms of pressure and temperature at various locations of the jet, they are adequately cooled by a circuit of demineralised water and make an arc of a circle driven by electric motors.

2.1.4 Model Support System

The "Model Support System" (MSS), is essentially an automated arm cooled by internal circuits of demineralised water and its function is related to the proper positioning of the model within the plasma jet.

The MSS allows a maximum vertical displacement equal to 1650 mm, and can also move in the longitudinal direction, helping to compensate for positioning errors with respect to the direction of flow of plasma. The support also allows a rotational movement and thus makes it possible to make tests in a dynamic manner.

2.1.5 Diffuser

The diffuser is designed to collect the flow of plasma out of the test chamber and slow down to subsonic speed values. It consists of a short convergent, followed by a long stretch of constant section and final section of duct diverts slightly upstream of the heat exchanger (Figure 7). Part of the converging section is located inside the test chamber.



Fig. 7. Diffuser

The geometry of the diffuser is summarized in Table.4:

Shape		Conical
Total length		49800 mm
Diameter	Converging	2650 mm
	Throat	2120 mm
	Diverging	2120 mm (min) - 3000 mm (max)
Parts	Converging	1
	Throat	4
	Diverging	2

Table 4. Diffuser geometrical data.

2.1.6 Heat exchanger

The heat exchanger is used to cool the flow of plasma from diffuser up to temperatures compatible with the operation of the vacuum system which is located just downstream.

This component consists of an input section cooled by an external circuit water tower, followed by tubes that run longitudinally in the conduit and exposed to direct current. They form the part that removes heat from the plasma.

Downstream of these tubes two circular sections of different diameters are placed that allow the connection to the vacuum system. There is also an expansion joint that allows to control the thermal deformation of the various components between the test chamber and heat exchanger.

2.1.7 Vacuum system

The function of the vacuum system is to maintain low pressure in the test chamber and it is located directly downstream of the heat exchanger (Figure 8).

The design specifications of the vacuum system are described in Table 5.

	Min	Max
Operating temperature (°C)	50	270
Operating inlet pressure (mbar)	0.35	15
Operating outlet pressure (mbar)	1013	1073

Table 5. Design specifications of the vacuum system

The vacuum system basically consists of three lines (plus an additional line called "by-pass line, which serves to maintain the vacuum in case of pressure fluctuations).

These three lines, which can provide different operating configurations depending on the level of vacuum that is required, are as follows:

- Line A: consists of 5 ejector in series (they are converging-diverging duct with circulating high temperature steam) and has a maximum capacity of 0.5 kg/s, it can work in conjunction with the other two lines;
- Line B: consists of four ejectors in series and has a maximum capacity of 1 kg/s;
- Line C: consists of three ejectors in series and has a maximum capacity of 2 kg/s.

The opening lines are controlled by corresponding on/off valves automatically controlled by the control system once set the conditions for conducting the test.



Fig. 8. Vacuum System

2.1.8 The DeNOx system

The DeNOx system serves to substantially reduce the percentage of nitrogen oxide (NO or NOx) inevitably present in the flow of plasma.

The DeNOx is essentially composed of two large reservoirs, "scrubber", which reduce the concentration of NO, a complex system of pumps, and three tanks. The first one is the largest and contains the washing solution, the second one contains sodium hypochlorite, NaOCl, and the third one contains caustic soda NaOH.

The DeNOx is able to maintain the concentration of nitric oxide (NO) below the limits fixed by the Italian law, and this is possible by means of a series of chemical reactions that occur within it.

2.1.9 Electrical system and power supply system

The system receives electricity from two external lines and it is equipped with an internal circuit for distribution. The power supply lines, through a complex system of processors, are reduced in a single line of industrial output voltage related to two different boxes: the first one is an electrical line of medium voltage (20 KV electrical system) which is connected to different users; a second cabin is the one of very high loads (32.5 kV, main load).

The cabin of the electrical system is designed to reduce the voltage and distribute electric power to the various units. It is equipped with four resin transformers powered with a medium voltage. The first two transformers make a conversion 20-0.4 KV providing power to the laboratories, while the remaining two transformers operating a conversion KV 20-6 feeding the engine and pump system. Inside the cabin, the power systems of the control system are installed, moreover an emergency instrumentation is present which ensures the supply of electricity in case of black-out. The Power Supply System is an independent unit and receives macro-command from the central system.

This unit provides electric power to the arc, up to a maximum of 70 MW. The subsystem is also equipped with appropriate filters suppressor of particular harmonics of the network.

The Power Supply System uses oil transformers which, depending on the required load current and voltage, may give rise to two different configurations: the first one guarantees 6000 at 20,250 V and the second one 9000 at 13500 V, the change of Configuration is done with remote-controlled pneumatic arms, which open or close certain circuits.

Downstream of the processors there are the current converters (AC / DC converter) that basically consist of thyristors cooled by demineralised water. Finally, the reactors have the task of eliminating the oscillations of the current (so-called "ripple"). The final closure of the circuit is done manually and, in cases of emergency, to disconnect the arch, a "Grow bar" that dissipates current through a coil is used. Finally, the "ballast resistors" are connected to the electrodes of the arc and are of the order of micro-ohm resistors, used to distribute the current.

2.1.10 Data Acquisition System and control system

The Data Acquisition System (DAS) is used to acquire data from sensors of various typologies. The instrumentation system is divided broadly into two classes: the first is called field instrumentation and is the set of sensors used for the acquisition of measurements relative to the facility, the second is named test instrumentation and refers to measurement on the models or inside the test chamber (for scientific targets).

In the electric arc there is a static pressure sensor appropriately certified, while there are no temperature gauges because any intrusive sensor that would measure temperatures of 10000 K would have problems immediately.

The basic functions of the acquisition system are both the measurement of thermodynamic parameters on the model (for example, to study the behaviour of materials during the return from a space mission) and the measurement of parameters related to plasma and aerothermodynamics and, in Test Leg for that purpose, the instrumentation is divided in "virtual instruments", that means installed outside the test chamber and therefore not intrusive, and "conventional instruments", i.e. inside the test chamber instrumentation (intrusive).

At the nozzle exit section there are four static pressure gauges, they are essentially four small holes in the order of half a millimetre in diameter spaced 90 degrees from each other, used to measure static pressure fluctuations in various positions. This situation is in fact indicative of a lack of uniformity of plasma.

Inside the test chamber there are four more pressure sensors, in addition to the two probes. The latter are basically two ways that are intended to measure the thermo-fluid dynamics characteristics of the flow in terms of stagnation pressure and heat flux on the surface of the probe exposed to the plasma.

The pressure sensors are small diameter holes using a suitable transducer that guarantees operation even in environments at low pressures.

In the next paragraph the heat flow meter in the stagnation point of the probe is described.

2.2 Heat flux measurement at the stagnation point

The heat flux is measured at the probe stagnation point by means of a Gardon gauge (Gardon, 1953) which is a heat flux sensor primarily intended for the measurement of high intensity radiation. It consists in a constantan foil hanging in a copper heat sink (see Figure

9). The foil is thermally and electrically connected to the copper cylinder through specific metallurgic techniques and it acts as first thermoelectrical material while the copper acts as the second thermoelectrical material. Thus, the foil and heat sink are respectively the hot and the cold joint of a thermocouple. A thin wire is then connected at the centre of the foil in order to generate a differential thermocouple which measures the temperature jump between the centre and the side of the foil.

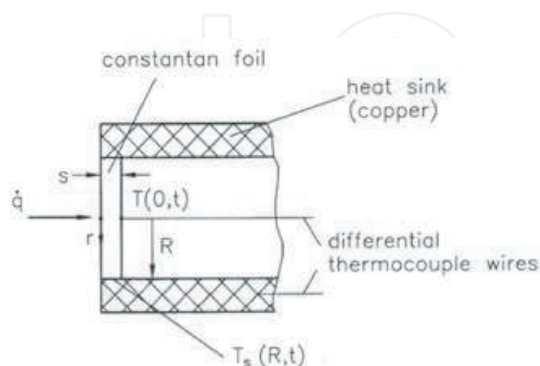


Fig. 9. Gardon gauge

In a polar coordinate system, the heat conduction equation can be written as:

$$\frac{\rho \cdot C_p}{K} \cdot \frac{\partial T}{\partial t} = \frac{1}{r} \cdot \frac{\partial T}{\partial r} + \frac{\partial^2 T}{\partial r^2} + \frac{\dot{q}}{s \cdot K} \quad (1)$$

where ρ , C_p , K and s are the density, the specific heat, the thermal conductivity and the thickness of the constantan foil, respectively, while \dot{q} is the heat flux acting at the centre of the foil.

Let us consider the following initial and boundary conditions:

$$\begin{aligned} T(r,0) &= T_s && \text{per } 0 < r < R \\ T(r,t) &= T_s && \text{per } 0 < t < \infty \end{aligned} \quad (2)$$

In the steady state regime and taking into account Eq.(2), the solution of Eq.(1) is:

$$\dot{q} = \frac{4sK}{(R^2 - r^2)} \cdot (T - T_s) \quad (3)$$

Thus, the heat flux at the centre of the foil ($r=0$) is:

$$\dot{q} = \frac{4sK}{R^2} \cdot (T - T_s) \quad (4)$$

Equations (3) and (4) show that the temperature jump between the centre and the side of the foil is proportional to the heat flux which then can be evaluated by measuring such temperature jump.

2.3 Specific total enthalpy measurement

The specific total enthalpy H_0 is computed through an energy balance in the arc heater and by using the following measurements: voltage, electrical current, gas mass flow rate, cooling

water flow rate and temperature jump of the cooling water. Once these quantities are measured, the specific total enthalpy is computed as follows:

$$H_0 = \frac{V \cdot I \cdot K - m_{H_2O} \cdot C_p \cdot \Delta T}{m_{gas}} \quad (5)$$

Where V is the potential difference between the ends of the arc heater, I is the electrical current, K is a conversion coefficient needed to keep consistent the units of measure, m_{H_2O} is the mass flow rate of the cooling water, C_p is the water specific heat and m_{gas} is the mass flow rate of the gas.

By using this approach and because of the uncertainty of the various measure instruments, the specific total enthalpy is estimated with an error which sometimes results notable. Such error can be computed by using Eq.(6).

$$\frac{dH_0}{H_0} = \frac{dV}{V} + \frac{dI}{I} + \frac{dm_{H_2O}}{m_{H_2O}} + \frac{d(\Delta T)}{\Delta T} - \frac{dm_{gas}}{m_{gas}} \quad (6)$$

3. SCIROCCO test procedure

The design of a test in a Plasma Wind Tunnel is complicated by the circumstance that many differences exist between flight and test chamber conditions (model size, dissociated flow conditions in test chamber, density level, etc.). All these aspects play an important role on the real gas non-equilibrium phenomena and make difficult the duplication of real flight conditions in wind tunnel. The main problem is to find the correct similitude parameters: to this effect, it is firstly needed to define the goal of the simulation, i.e. the phenomenon we are interested in reproducing; this is often a flight condition to be simulated on the test article in wind tunnel, but it can be a particular customer's request as well (Marini et al. 2007). Hence, the design of ground-based experiments, as well the interpretation of experimental data, needs an appropriate support of numerical simulations. As matter of fact, in order to meet the specific test requirements (Stagnation heat flux, stagnation pressure, test time and test article size), Computational Fluid Dynamics (CFD) calculations are needed to accurately design the configuration of the facility. Successively, a structural safety analysis is carried out with the aim of verifying the structural integrity of the test article. After the test is performed and experimental data are acquired, numerical activities are again needed to rebuild the test and to support in the interpretation of the test results. Moreover, the ability of the developed finite element model in predicting the temperature field in the test article is verified by comparing numerical data with experimental one.

The present paragraph deals with the description of the procedure for the execution of a test in the facility SCIROCCO. An overview of the test procedure is given in the flow chart of Figure 10.

Each steps of such procedure will be described in detail hereafter:

Requirements: The first aspect that is taken into account when a test in SCIROCCO is designed is the definition of the requirements.

Requirements can be formulated in terms of heat flux (more often), or in terms of pressure, temperature or they can also be formulated in terms of scientific phenomena reproduction such as shock wave -boundary layer interaction and so on.

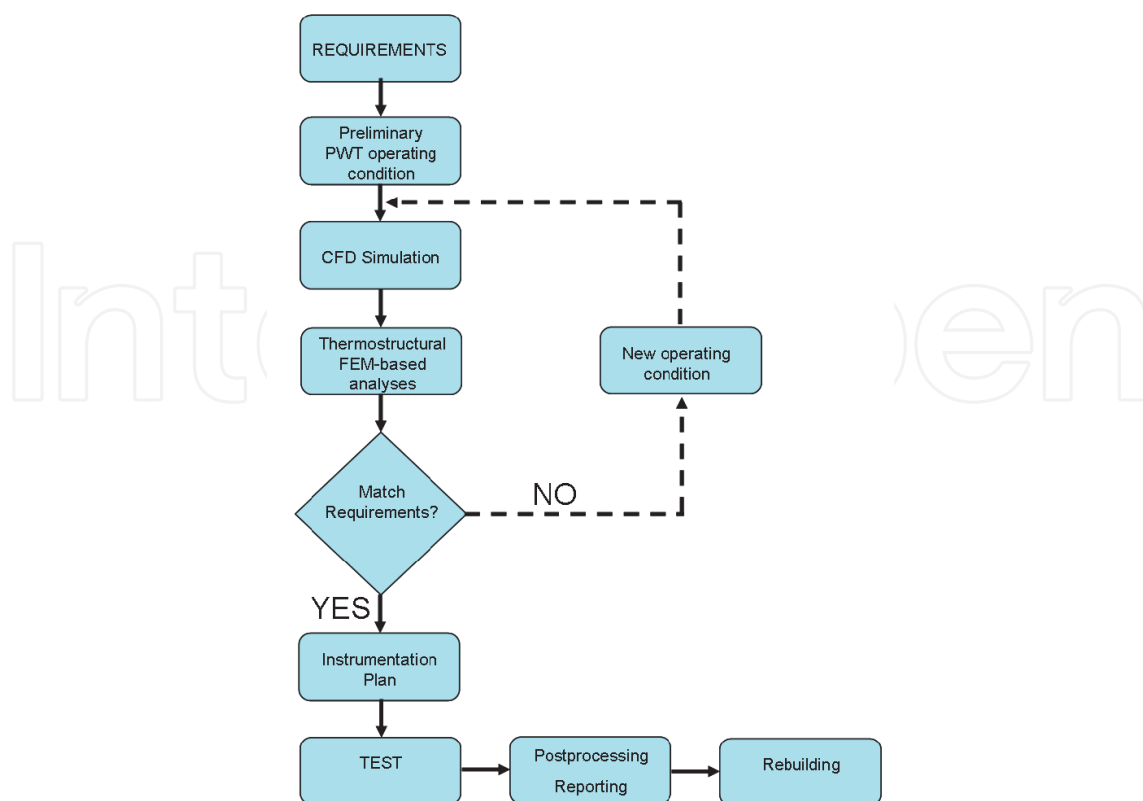


Fig. 10. SCIROCCO Test Procedure

The requirements are given by the customer and a process of trade-off begins. Indeed a feasibility study verifies the compatibility of both test requirements with the PWT theoretical envelope and test article dimensions with test chamber capability, in order to avoid blockage phenomenon. Then, a first operating condition is defined by means of both engineering tools, to derive the stagnation point heat flux and pressure from requirements on the test article, and the curve-fit calibration law for fast PWT Test Setting (De Filippis et al. 2003).

Preliminary PWT operating condition: Once the first operating condition has been defined, the driving parameters of the facility (current and air mass flow) and the PWT performances in terms of reservoir pressure (P_0) and reservoir enthalpy (H_0) are obtained, and consequently the stagnation pressure (P_s) and stagnation heat flux (Q_s) on the PWT calibration probe are evaluated.

CFD Simulations: Starting from the preliminary condition, the final PWT settings able to match the test requirements are defined by means of an iterative procedure, which involves both CFD computations and evaluations with simplified engineering correlations.

Free stream conditions to be used for the simulation of the flow around the model in the test chamber are obtained from the numerical computation of the nozzle flow. If the CFD simulation of the flow past the model shows that test requirements over the model are not still achieved, a new reservoir condition (P_0 , H_0) is deduced by using simplified engineering correlations and the procedure restarts from the CFD simulation of the nozzle flow. As an alternative, test requirement fulfilment could be reached with the same reservoir conditions, properly modifying the model position inside the test chamber and/or the model attitude. In this last hypothesis only model computation has to be iterated.

Once the final PWT operating condition has been defined, simulation of the flow past the PWT calibration probe provides pressure (P_s) and heat flux (Q_s) at the probe stagnation point. These values, measured during the test, ensure the achievement of the desired operating condition in terms of (P_0, H_0) in test chamber.

Thermostructural FEM-based analysis: once the PWT operating condition ensuring the achievement of test requirements has been identified, the structural integrity of the model under that conditions has to be verified. At this stage a FEM transient thermal analysis is carried out by applying on the model the heat flux distribution (usually multiplied by a safety coefficient equal to 1.2) computed by CFD simulations. The thermal analyses are highly nonlinear since radiation to the environment must be taken into account. The temperatures predicted by the FE model are checked against the temperature limits of the materials under investigation. Critical instants are then identified as those ones at which high gradients of temperature (and thus high thermal stresses) are expected. Nonlinear static structural analyses are then carried out by applying the temperature field predicted at the critical instants as a structural load. FE codes able to perform non linear contact analyses are used at this stage. Thermal and structural simulations are very useful also to identify critical parts which have to be properly monitored during the tests. In other words, expected temperatures predicted by numerical simulations are the input data for the test instrumentation plan whose objective is accurately choose the kind of instruments, their location and range, that are used to monitor the test and to reach its scientific aim.

Instrumentation plan: When the trade-off phase for the definition of the test conditions is concluded, the instrumentation setup to be used for the test is designed. Indeed, the particular environment typical of hypersonic regime and the scientific aims of the tests require a number of parameter measurements. Hence, different kind of instruments, both intrusive (thermocouples) and not intrusive (pyrometers and thermocameras), measuring at different locations have to be properly chosen.

Similarly to the test conditions definition phase, a trade-off phase for the definition of the instrumentation is performed, at the end of which the instrumentation plan is made, that is a design report containing all the information about the test instrumentation.

Test execution and post processing reporting: Once the test conditions (including test duration and all the other parameters) and the test instrumentation are fixed, the test is executed. After the test a period of time is necessary for the post processing (data treatment) and the reporting, at the end of which a complete report, the "Test Report", is carried out.

In this document all the information about the test and all the instrumentation measured and treated data are reported.

Rebuilding: The numerical rebuilding is another important phase, that, differently from all the other phases, follows the test itself. It is performed starting from the measured values of stagnation heat flux and pressure rather than the values of reservoir pressure and enthalpy, and its aim is to provide a meaningful heat flux distribution on the model during the test as input for the thermo-structural rebuilding analysis, whose results (wall temperature distribution) can be compared with the IR thermo-graphic acquisition generally performed in PWT tests.

From a numerical point of view it determines the condition (P_0, H_0) that provides the better agreement with the probe measurements and then, with the same condition, the heat flux over the model is recomputed.

4. Rebuilding of a nose cap demonstrator

In order to show the importance of “rebuilding” a PWT test, this step will be presented in detail referring to a specific application.

Within the context of the research project Sharp Hot Structures (SHS), focused on the assessment of the applicability of Ultra High Temperature Ceramics (UHTCs) to the fabrication of high performance and sharp hot structures for reusable launch vehicles, the nose cap demonstrator named Nose_2 was tested in the SCIROCCO Plasma Wind Tunnel. The architecture of the nose is shown in Figure 11. The basic idea of the Nose_2 design was to couple conventional C/SiC materials to novel Ultra-High Temperature ZrB₂-SiC Ceramics (UHTC) in order to create a multi-material structure able to withstand the severe condition associated with slender-shaped hot structures and non-conventional reentry mission profiles. The nose is made of two main components: the tip and the dome.

The conical tip, which was intended to sustain the greatest thermal load in the whole nose cap structure, was made of ultra-high temperature ZrB₂-SiC ceramic. The tip was produced by hot pressing sintering and then finished by EDM (Electrical Discharge Machining). The outer dome was made of C/SiC and has the shape of a hollow frustum of cone. It was manufactured by Polymer Infiltration and Pyrolysis (PIP) process. A ZrB₂-SiC coating, about 500 μm thick, was applied by Plasma Spray Deposition technique on the external surface of the outer dome to protect the fibres from oxidation.

The inner dome was made of graphite and its main function was to increase the thermal capacity of the system. A mechanical interface in AISI304 allowed the connection between the nose cap demonstrator and the Model Support System.

Finally, the coupling between tip and dome of the nose cap was guaranteed by a coupling pin in titanium alloy which was preloaded by a spring. One end of the pin was not axial-symmetric and it was introduced into the hole and then rotated by 90 degrees in order to ensure the contact. The coupling hole dimensions are the results of a sensitivity analysis (Ferraiuolo et al., 2008) performed with the aim to reduce stress concentration next to the coupling hole of the tip component and, at the same time, to reduce the massive volume taken away by spark erosion. The bend radius, the entire length and the diameter of the hole were chosen as parameters of the sensitivity analysis.

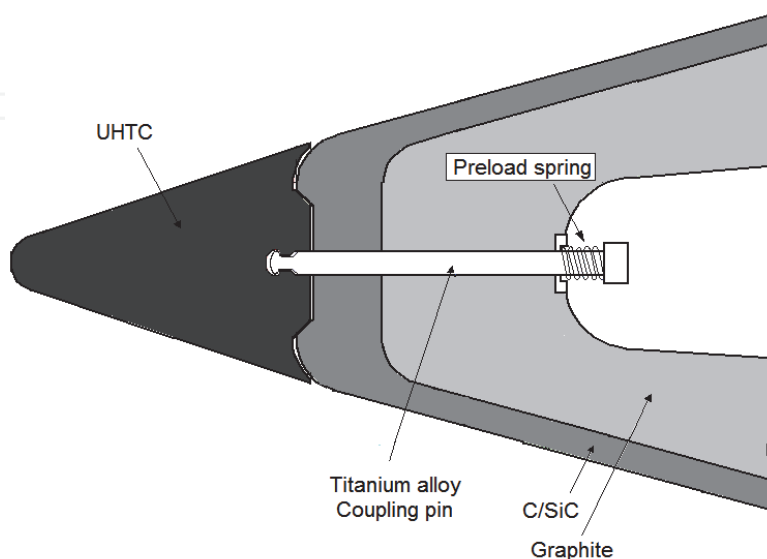


Fig. 11. Schematization of tip-dome coupling

In Figure 12, the experimental data, in terms of temperature curves measured by an IR thermocamera along the nose profile and at several time steps, are shown. Experimental data were not available within the range $[x=0, x=0.025\text{m})$ since this area was characterized by a low view factor with respect to the IR thermocamera.

The enthalpy (H_0) and the pressure (P_0) at the stagnation point measured during the experimental test were 13.5 MJ/Kg and 1.9 bar, respectively. These data were used by CFD simulation to compute the heat flux distribution acting on the nose cap during the test.

The change in manufacturing process passing from coupon level to sub-component level makes it very difficult to determine some experimental parameters which are needed in numerical computations. One of these experimental parameters is the catalysis of the UHTC. Hence, in order to verify the influence of catalysis on the thermal behaviour of the nose cap, both the Non-Catalytic Wall (NCW) model and the Finite Rate Catalysis (FRC) one were used to compute heat fluxes acting on its external surface.

The heat flux distributions computed by using the two different catalysis models are shown in Figure 13 where the profile of the nose (red curve) is also represented. The stagnation heat flux, that is the heat flux computed for $x=0$ and $y=0$, for the NCW and FRC catalysis models were found respectively to be 1310 kW/m² and 1490 kW/m². However, because of the uncertainty in the measurements of both the probe stagnation heat flux and the probe stagnation pressure (measurements that affects the CFD calculations), the heat flux distributions plotted in Figure 13 were estimated with an uncertainty equal to $\pm 8.9\%$.

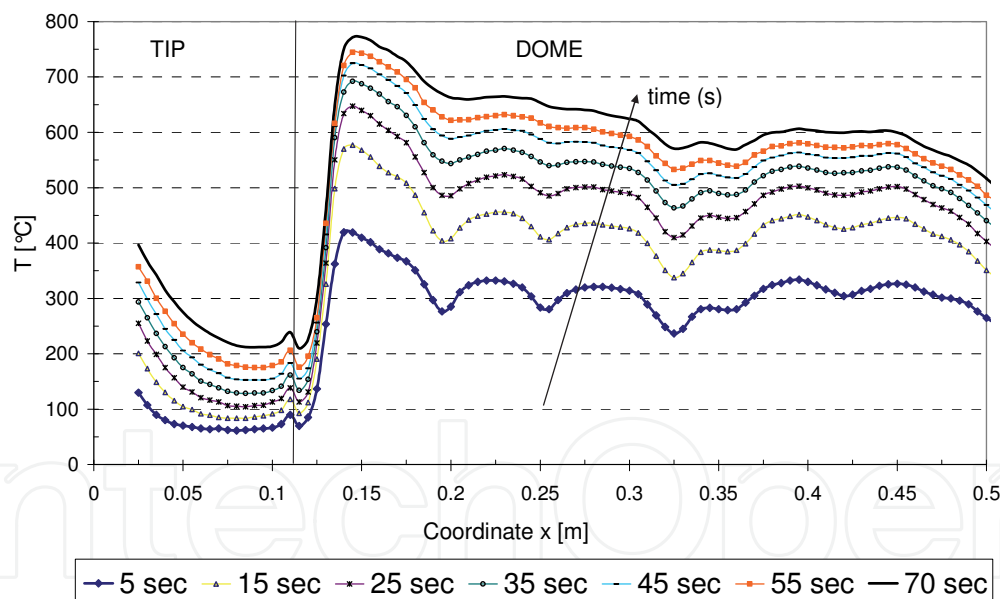


Fig. 12. Experimental temperature curves at several time steps

A 3D FE model (Figure 14) was built by using the FE commercial code ANSYS which was found able to deal with these thermo-mechanical problems. The heat flux distribution computed via CFD simulation was applied on the exposed external surfaces and, in order to reproduce the same conditions occurred in the PWT during the experimental test, heat fluxes were applied constantly for 72s, then they were set to zero to simulate the cooling. The duration and the heat fluxes magnitude are representative of a re-entry trajectory which was one of the requirements of the nose design. The radiation to the environment was taken into account in the FE model.

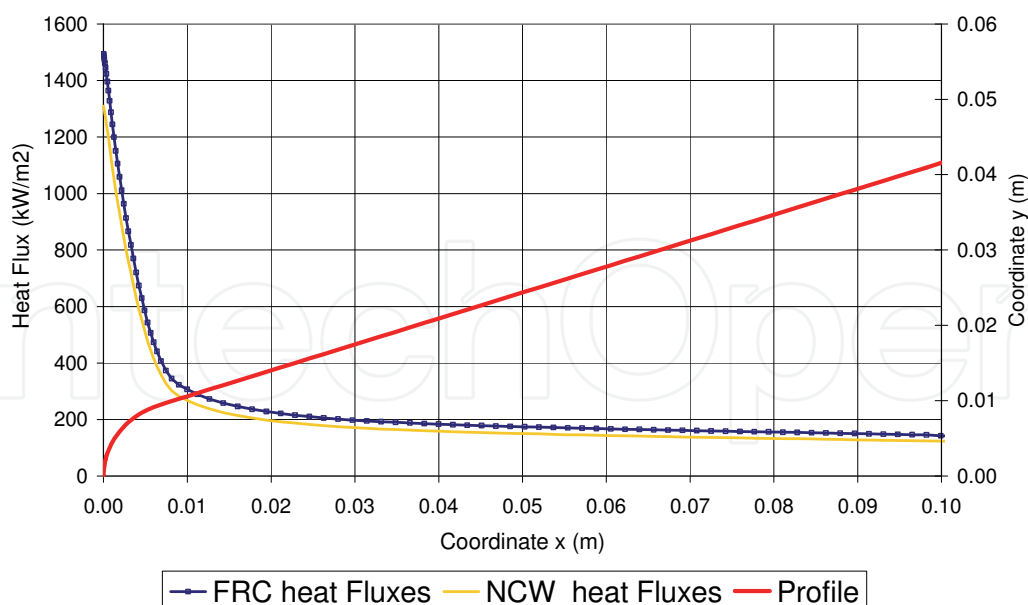


Fig. 13. Heat flux distribution on the profile of the nose

In Figure 15 the numerical temperature curve, predicted on the tip profile and obtained by applying NCW heat fluxes, is compared to that one obtained by applying FRC heat fluxes. The plotted curves are predicted at time 50s of the simulation and they are compared to the experimental data registered at same time instant. The NCW model was found to provide better agreement with experimental data with respect to the FRC model and was adopted for the rest of this research work.

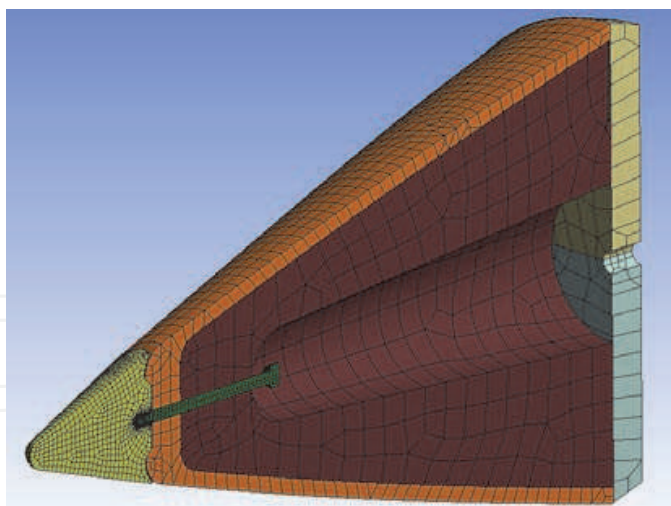


Fig. 14. Section of the 3D FE model

After the test, in the post-processing phase, it was found that the dome surface temperature was higher than the tip surface temperature, though the heat flux acting on the tip was considerably higher as shown in Figure 13. In order to interpret so high temperatures measured on the dome surface, a numerical study was performed. Such study was just qualitative and was focused to the improvement of knowledge on the physical phenomenon under investigation. In particular, two different simulations, with two different assumptions

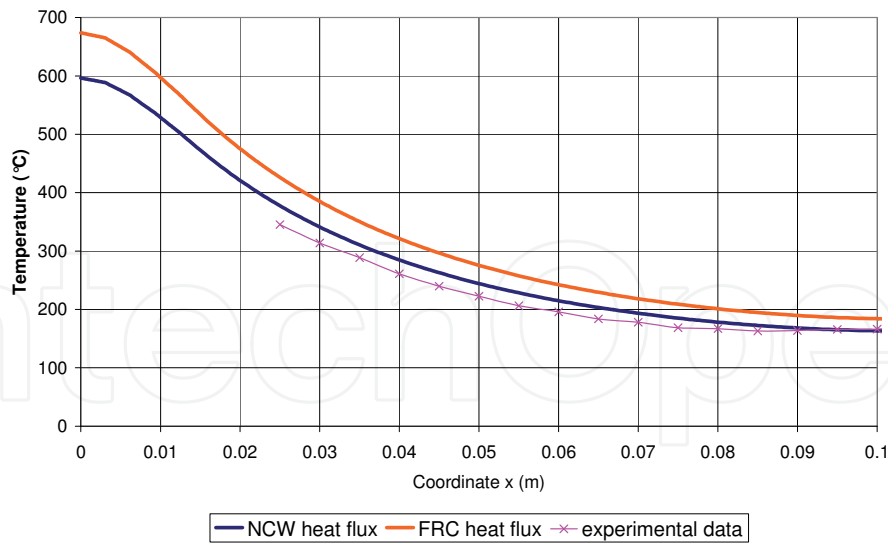


Fig. 15. Comparison between numerical and experimental tip surface temperature at 50s.

on the modelling of the C/SiC-coating interface, were carried out. Comparison between temperatures predicted by the two simulations at time 70s and those measured during the test at the same time instant are shown in Figure 16. In the first simulation, the coating layer was assumed perfectly bounded to the C/SiC, hence it was not modelled because its thermal resistance was assumed negligible. The strong discrepancy between experimental temperatures measured at the outside of the dome and those predicted by this simulation justified further investigations to better understand how to model the C/SiC - coating interface. Therefore, in the second simulation the coating layer was assumed completely detached from the C/SiC, hence it was modelled by a thin surface completely not in contact with the C/SiC, in such a manner the coating was not able to transfer heat to the C/SiC by conduction but only by internal radiation.

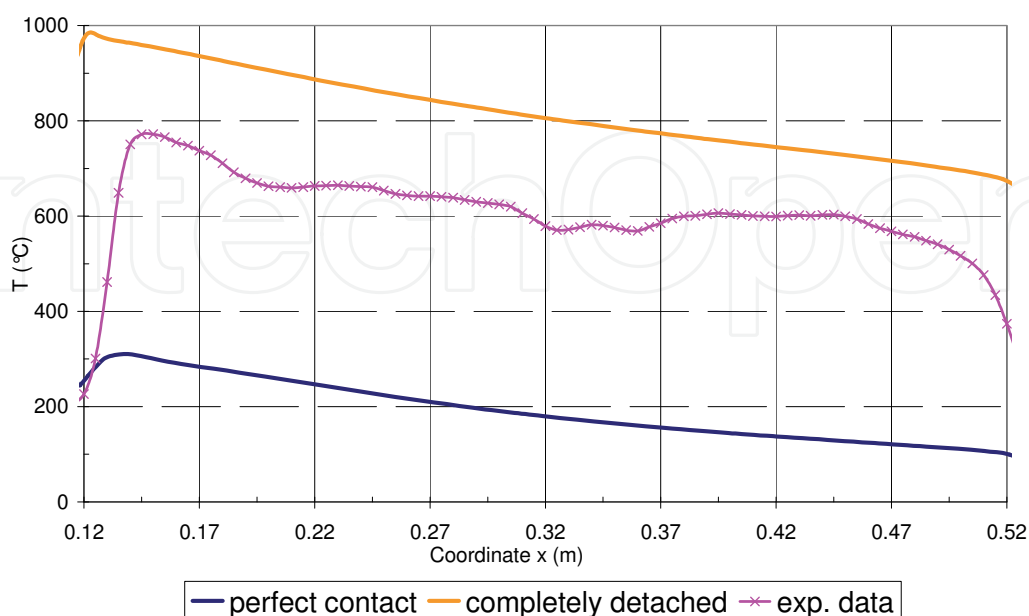


Fig. 16. Comparison between numerical and experimental dome surface temperature at 70s.

Temperatures predicted in the case of coating completely detached are closer to the experimental data with respect to those predicted in the case of perfect contact suggesting that most likely the contact between the coating and C/SiC during the PWT test was neither perfect nor completely separated but local detachments occurred in unknown regions of the interface. The wavy trend of the experimental temperatures confirms this hypothesis. Indeed, where the detachment occurred, the coating was not able to transfer heat to the C/SiC and a peak in temperature was measured by the IR thermocamera. On the other hand, where the contact was perfect, the heat was drained towards the inner dome and a lower temperature value was registered. Destructive inspections confirmed later that the coating was locally detached by the outer dome in several zones.

Further investigations were made during the rebuilding phase of a second PWT test performed on the same nose cap demonstrator (Borrelli et al., 2010). Experimental data were compared with numerical results in order to help in interpreting the experimental test itself. The knowledge on the physical phenomenon under investigation was greatly improved thanks to the synergy between numerical and experimental activities. In particular, a qualitative study of the modeling of the tip-dome interface was performed in order to estimate the thermal contact resistance that heat flux encounters in passing through the demonstrator. Modeling this interface as imperfect greatly improved the accuracy of the numerical predictions.

5. Conclusion

A brief introduction on the characteristics of a plasma wind tunnel facilities, as well as their performances and applications, was provided. Particular attention was given to the SCIROCCO PWT facility, that is the plasma wind tunnel developed by CIRA, which is the World's most powerful ground test facility. Successively, each step performed for the success of a plasma wind tunnel test was examined in detail. In particular, the synergy between the experimental team and the numerical one in each step of the test procedure was stressed by providing explanatory examples.

6. Acknowledgment

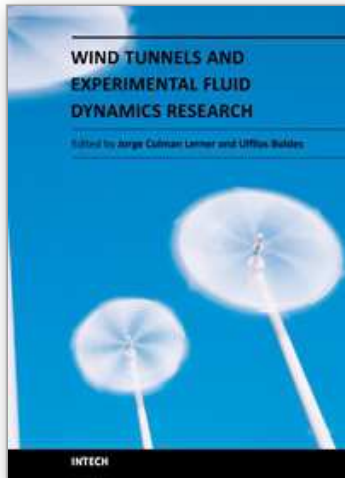
The authors would like to thank the entire CIRA PWT staff for providing useful information needed to write this work.

7. References

- Borrelli, R.; Riccio, A.; Tescione, D.; Gardi, R. & Marino, G. (2010). Numerical/Experimental Correlation of a Plasma Wind Tunnel Test on a UHTC-made Nose Cap of a Reentry Vehicle, *Journal of Aerospace Engineering*, Vol.23, No.4, pp. 309-316, ISSN 0893-1321
- De Filippis, F.; Caristia, S.; Del Vecchio, A. & Purpura C. (2003). The Scirocco PWT Facility Calibration Activities, *3rd International Symposium Atmospheric Reentry Vehicle and Systems*, Arcachon, France.
- Ferraiuolo, M.; Riccio, A.; Tescione, D.; Gardi, R. & Marino, G. (2008). Contact Sensitivity Analysis of a Coupling Pin for the Nose Cap of a Launch of a Re-entry Vehicle, *Journal of the Interplanetary Society*, Vol.61, pp. 14-19, ISSN 0007-084X

- Gardon, R. (1953). An Instrument for the Direct Measurement of Intense Thermal Radiation. *Review of Scientific Instruments*, Vol.24, pp. 366-370.
- Kelly, H. N.; Rummeler, D. R. & Jackson, R. (1983). Research in Structures and Materials for Future Space Transportation Systems - An Overview. *Journal of Spacecraft and Rockets*, Vol.20, No.1, pp. 89-96, ISSN 0022-4650
- Marini, M.; Di Benedetto, S.; Rufolo, G. C.; Di Clemente, M. & Borrelli, S. (2007). Test Design Methodologies for Flight Relevant Plasma Wind Tunnel Experiments, *Proceedings of West-East High Speed Flow Field Conference*, Moscow, Russia
- Shih, P. K.; Prunty, J. & Mueller, R. N. (1988). Thermostructural Concepts for Hypervelocity Vehicles. *AIAA paper*, No. 88-2295
- Thornton E. A. (1996). *Thermal Structures for Aerospace Applications*, AIAA, ISBN 1-56347-190-6, Reston, Virginia.

IntechOpen



Wind Tunnels and Experimental Fluid Dynamics Research

Edited by Prof. Jorge Colman Lerner

ISBN 978-953-307-623-2

Hard cover, 709 pages

Publisher InTech

Published online 27, July, 2011

Published in print edition July, 2011

The book “Wind Tunnels and Experimental Fluid Dynamics Research” is comprised of 33 chapters divided in five sections. The first 12 chapters discuss wind tunnel facilities and experiments in incompressible flow, while the next seven chapters deal with building dynamics, flow control and fluid mechanics. Third section of the book is dedicated to chapters discussing aerodynamic field measurements and real full scale analysis (chapters 20-22). Chapters in the last two sections deal with turbulent structure analysis (chapters 23-25) and wind tunnels in compressible flow (chapters 26-33). Contributions from a large number of international experts make this publication a highly valuable resource in wind tunnels and fluid dynamics field of research.

How to reference

In order to correctly reference this scholarly work, feel free to copy and paste the following:

Rosario Borrelli and Adolfo Martucci (2011). SCIROCCO Plasma Wind Tunnel: Synergy between Numerical and Experimental Activities for Tests on Aerospace Structures, Wind Tunnels and Experimental Fluid Dynamics Research, Prof. Jorge Colman Lerner (Ed.), ISBN: 978-953-307-623-2, InTech, Available from: <http://www.intechopen.com/books/wind-tunnels-and-experimental-fluid-dynamics-research/scirocco-plasma-wind-tunnel-synergy-between-numerical-and-experimental-activities-for-tests-on-aeros>

INTECH
open science | open minds

InTech Europe

University Campus STeP Ri
Slavka Krautzeka 83/A
51000 Rijeka, Croatia
Phone: +385 (51) 770 447
Fax: +385 (51) 686 166
www.intechopen.com

InTech China

Unit 405, Office Block, Hotel Equatorial Shanghai
No.65, Yan An Road (West), Shanghai, 200040, China
中国上海市延安西路65号上海国际贵都大饭店办公楼405单元
Phone: +86-21-62489820
Fax: +86-21-62489821

© 2011 The Author(s). Licensee IntechOpen. This chapter is distributed under the terms of the [Creative Commons Attribution-NonCommercial-ShareAlike-3.0 License](#), which permits use, distribution and reproduction for non-commercial purposes, provided the original is properly cited and derivative works building on this content are distributed under the same license.

IntechOpen

IntechOpen